

Comprehensive Edge Detection Algorithm for Satellite Images

¹Abhishek Gudipalli and ²Ramashri Tirumala

¹School of Electrical Engineering, VIT University, Vellore - 632014, India

²Department of Electronics and Communication Engineering,
Sri Venkateswara University College of Engineering, Tirupati - 517501, India

Abstract: Edges are prominent features in images and their analysis and detection are an essential goal in computer vision and image processing. Indeed, identifying and localizing edges are a low level task in a variety of applications such as 3-D reconstruction, shape recognition, image compression, enhancement and restoration. In this paper, we considered edge detection as one of the technique and the evaluation metrics such as SSIM (Structural Similarity Index) and VIF (Visual Information Fidelity) has been applied to the images to measure the image quality. In this paper Satellite images with natural-color are considered, which are captured from the Moderate Resolution Imaging Spectroradiometer (MODIS) on NASA's Terra satellite. In the present work evaluation metrics are applied to the original image and edge detected image, thus from experimental results it is observed that the proposed algorithm works well for measuring the quality of hyper spectral images.

Key words: Edge detection • Satellite images • MODIS • Color models • SSIM • VIF

INTRODUCTION

Edge detection is an important fundamental pre-processing step and is used as an image processing tool in many edge detection applications. Edges map have a significant role in application such as image categorization, image registration, feature extraction and pattern recognition [1]. An edge detector is also a mathematical operator that responds to the spatial change and discontinuities in gray levels of pixel set in an image [1]. Each industry will use its suitable color model, for example CMYK for printing, YUV for video systems and so on. Satellite images find extensive applications in the fields of meteorology, landscape, regional planning, agriculture, geology, forestry, biodiversity conservation, education, intelligence and warfare. Images can be in visible color models or in other color models. In remote sensing applications, interpretation and analysis of satellite imagery is conducted using specialized image processing software [2, 3, 4]. Thus in this paper we apply edge detection techniques to a satellite images with natural-color. The RGB image is transformed to various color models such as YUV, YCbCr and XYZ [5, 6]. The metrics such as SSIM and VIF have been applied to the

above models for assessment of quality of images and out of these XYZ color model is providing more detailed edge information than the other color models.

Different Color Spaces

YUV and YCbCr Color Models: The YCbCr color space is used for component digital video is a scaled and offset version of the YUV color space. The YUV color model is the basic color model used in analogue color TV broadcasting. Initially YUV is the re-coding of RGB for transmission efficiency (minimizing bandwidth) and for downward compatibility with black-and white television. The YUV color space is "derived" from the RGB color space. It comprises of the *luminance* (Y) and two color difference (U,V) components. The luminance can be computed as the weighted sum of the Red, Green and Blue components, the color difference, or *chrominance*, components are formed by subtracting luminance from blue and from red. The principal advantage of the YUV model in image processing is decoupling of luminance and color information. The importance of this decoupling is that the luminance component of an image can be processed without affecting its color component. For example the histogram equalization of the color image in

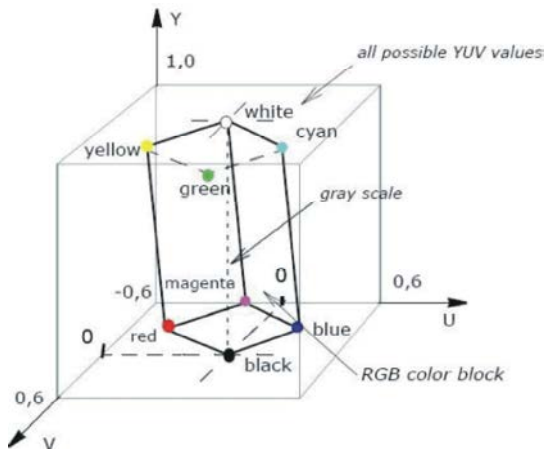


Fig. 1: RGB colors cube in the YUV color space

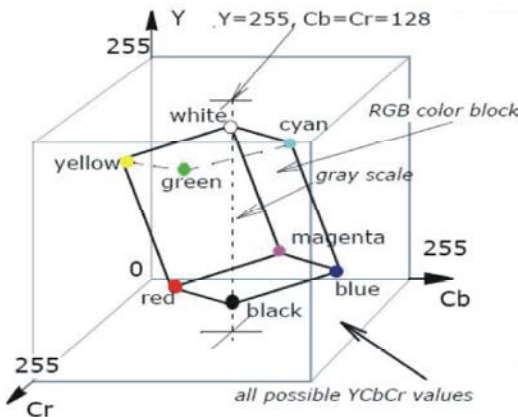


Fig. 2: RGB colors cube in the YCbCr color space

the YUV format may be performed simply by applying histogram equalization to its Y component. There are many combinations of YUV values from normal range that result in invalid RGB values, because the possible RGB colors occupy only part of the YUV space limited by these ranges. Figure 2 shows the valid color block in the YUV space that corresponds to the RGB color cube RGB values are normalized to [0..1] [7].

The Y'U'V' notion means that the components are derived from the gamma corrected R'G'B'. Weighted sum of these non linear components forms a signal representative of the luminance called *luma* Y' (*luma* is often loosely referred to as *luminance* so you need to be careful to determine whether a particular author assigns a linear or a non-linear interpretation to the term *luminance*). [7] The YCbCr color model is a scaled and offset version of the YUV color space and is used for component digital video. The position of the block of RGB-representable colors in the YCbCr space is shown in Figure 2.1 RGB Colors Cube in the YCbCr Color Model [7].

Conversion Between RGB and YUV Models:

$$Y' = 0.299 * R' + 0.587 * G' + 0.114 * B'$$

$$U' = -0.147 * R' - 0.289 * G' + 0.436 * B' = 0.492 * (B' - Y')$$

$$V' = 0.615 * R' - 0.515 * G' - 0.100 * B' = 0.877 * (R' - Y')$$

Conversion Between RGB and YCbCr Models:

$$Y' = 0.257 * R' + 0.504 * G' + 0.098 * B' + 16$$

$$Cb' = -0.148 * R' - 0.291 * G' + 0.439 * B' + 128$$

$$Cr' = 0.439 * R' - 0.368 * G' - 0.071 * B' + 128$$

CIE XYZ Color Model: The XYZ color space is an international standard developed by the CIE (Commission Internationale de l'Eclairage) [7]. This model is based on three hypothetical primaries, XYZ and all visible colors can be represented by using only positive values of X, Y and Z. The CIE XYZ primaries are hypothetical because they do not correspond to any real light wavelengths. The Y primary is intentionally defined to match closely to luminance, while X and Z primaries give color information. The main advantage of the CIE XYZ space (and any color space based on it) is that this space is completely device-independent. The position of the block of RGB-representable colors in the XYZ space is shown in Figure3 RGB Colors Cube in the XYZ color space [7].

Conversion Between RGB and XYZ Models:

$$X = 0.412453 * R + 0.35758 * G + 0.180423 * B$$

$$Y = 0.212671 * R + 0.71516 * G + 0.072169 * B$$

$$Z = 0.019334 * R + 0.119193 * G + 0.950227 * B$$

Satellite Images – Dust Storms: Dust storms can be a relatively common meteorological phenomenon in arid and semi-arid regions of the world [8]. They arise when a gust front passes or when the wind force is strong enough to remove loose sand and dust from the dry soil surface [8]. The result is formation of wall of sand that can obscure visibility within seconds. In the world, the major dust storms arise in the Sahara desert and arid lands around the Arabian Peninsula. In Asia, the Gobi desert is a major source. Annually, these storms carry more than 3 billion metric tons of dust aloft into the atmosphere [8]. Between May and October, strong winds blow off the Sahara desert and the west coast of north Africa, carrying soil and dust westward across the Atlantic ocean [8]. Today, these storms are becoming of more concern as worldwide deforestation, overgrazing and climate change combine to generate massive dust clouds that can carry particles aloft [8].

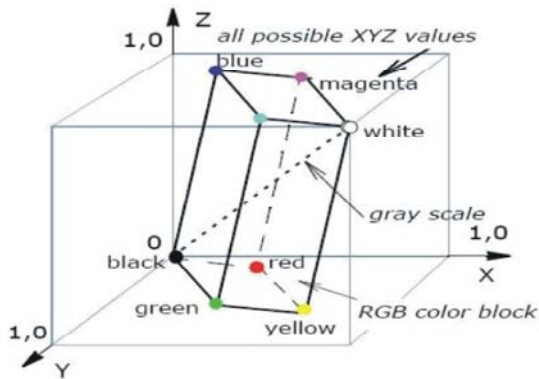


Fig. 3: RGB colors cube in the XYZ color space

NASA designs and launches set of Earth Observing System (EOS) satellites, each with several sensors [9]. NASA considers most of these to be research instruments and the data are generally provided at no charge through one of eight Earth Science Distributed Active Archive Centers (DAACs). The MODIS sensor, located on the Terra (and Aqua) satellite platforms, has 36 spectral channels [9]. It was designed to provide a wide variety of information about land, oceanic and atmospheric conditions [9]. MODIS has good spatial (250 m–1km horizontal) and temporal (1-2 day) resolution. With the large number of spectral bands and the ability to use this spectral information to derive biogeophysical results, the MODIS science team has developed 44 products (processed data sets) for a range of observations [9]. The data products used in this study were: MOD021KM-Level-1B with 1 km resolution, used to produce red-green-blue (RGB) “true color” imagery and conduct qualitative analysis and MOD04-Level 2 provides on aerosol optical depth, mass concentration and cloud fraction, for both qualitative and quantitative analysis [9]. For air quality, the two main DAACs providing data are located at NASA Goddard Space Flight Center and NASA Langley Research Center [9].

Evaluation Metrics: In image processing applications, the measurement of image quality plays main role. Image quality assessment algorithms are classified into three categories: FullReference (FR), Reduced-Reference (RR) and No-Reference (NR) algorithms [10]. True No Reference algorithms are difficult to design and little progress has been made (Sheikh *et al.*, 2005). Full Reference algorithms are easier to design and The SSIM index is a full reference metric. In this, the measurement of image quality is based on reference image of perfect quality. SSIM is designed to improve Peak Signal-to-Noise Ratio (PSNR) and Mean Squared Error (MSE),

which is proved to be inconsistent with human eye perception [11]. However, in RR or NR quality assessment, partial or no reference information is available. The SSIM index is defined as [11]:

$$SSIM(x,y) = \frac{\sigma_{xy} + C_1}{\sigma_x \sigma_y + C_1} \cdot \frac{2\mu_x \mu_y + C_2}{\mu_x^2 + \mu_y^2 + C_2} \cdot \frac{2\sigma_x \sigma_y + C_3}{\sigma_x^2 + \sigma_y^2 + C_3} \quad (1)$$

Let x and y be the two discrete non-negative signals extracted from the same spatial location from two images being compared, respectively μ_x , σ_x^2 and σ_{xy} be the mean of x , the variance of x and the covariance of x and y , respectively. μ_x and σ_x gives the information on luminance and contrast of x . σ_{xy} measures the structural similarity.

where C_1 , C_2 and C_3 are small constants given by $C_1 = (K_1 L)^2$; $C_2 = (K_2 L)^2$ and $C_3 = C_2 / 2$; respectively. L is the dynamic range of the pixel values ($L = 255$ for 8 bits/pixel gray scale images) and $K_1 < 1$ and $K_2 < 1$ are two scalar constants [11].

Sheikh and Bovik (2006) developed a visual information fidelity (VIF) index for Full Reference measurement of quality of image. VIF is calculated between the reference image and its copy [12]. For ideal image, VIF is *exactly* unity. For distorted image types, VIF lies in between interval [0, 1]. Let $e=c+n$ be the reference image and n zero-mean normal distribution $N(0, \sigma_v^2 I)$ noise. Also, let $f=d+n'=gc+v'+n'$ be the test image, where g represents the blur, v' the additive zero-mean Gaussian white noise with covariance $\sigma_v^2 I$ and n' the zero mean normal distribution $N(0, \sigma n^2 I)$ noise [12]. Then, VIF can be computed as the ratio of the mutual information between c and f and the mutual information between c and e for all wavelet subbands except the lowest approximation subband [12].

$$VIF = \frac{\sum I(c; f | z)}{\sum I(c; e | z)} \quad (2)$$

Proposed Edge Detection Algorithm: The proposed algorithm can be explained in seven steps:

Step 1: The RGB image is sub divided into R, G and B layers of the image.

Step 2: A 3X3 Laplacian mask is convolved with the R component of the image.

Step 3: The edge detected R and the G, B layers of the image are concatenated to obtain edge detected image

Step 4: SSIM and VIF values are calculated between the R edge detected image and RGB image.

Table 1: SSIM and VIF Values for RGB, XYZ, YCbCr and YUV images

COLOR MODEL	SSIM	VIF
RGB	0.6243	0.4958
XYZ	0.6514	0.5579
YCbCr	0.5999	0.5484
YUV	0.4203	0.6293

Step 5: Repeat steps 2 to 4 to calculate the SSIM and VIF values between G edge detected image and RGB image

Step 6: Repeat steps 2 to 4 to calculate the SSIM and VIF values between B edge detected image and RGB image

Step 7: The SSIM and VIF values of individual components are averaged.

Step 8: R, G and B values of the image are transformed into its YCbCr, YUV and XYZ Intensity values using the conversion formulas.

Step 9: Repeat steps 1 to 8 to calculate SSIM and VIF values for YCbCr, YUV and XYZ images.

Experimental Results: The Proposed algorithm has been applied to satellite images of different color models and SSIM & VIF values are computed for a set of edge detected images and dataset is formed and tabulated in Table 1. The natural color image was captured when dust blew over Sudan in mid-May 2013 by the Moderate Resolution Imaging Spectroradiometer (MODIS) on NASA’s Terra satellite [13]. The dust plume may have arisen from fine lake and riverbed sediments and extended hundreds of kilometers, thick enough in places to completely hide the land surface below. Dust storms count among the most frequent natural hazards in this dry country [13].

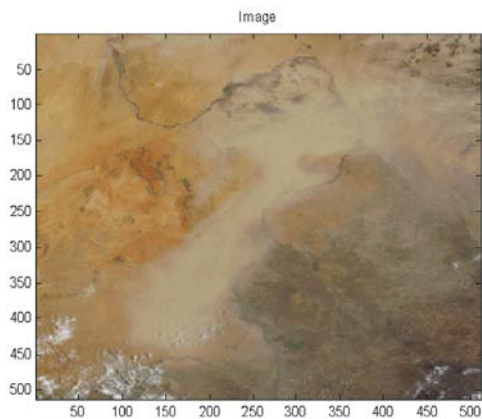


Fig. 4: RGB image



Fig. 5: RGB edge detected image

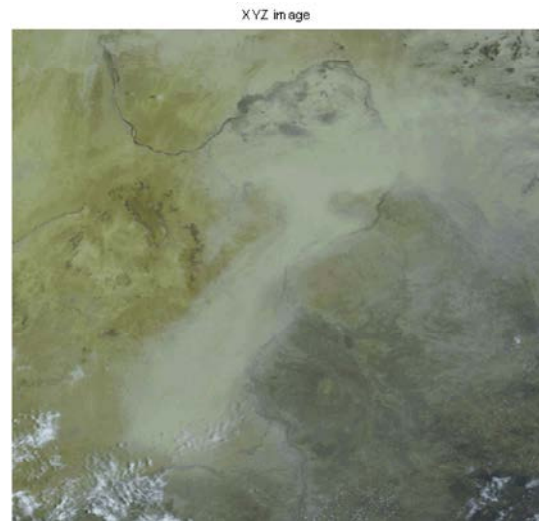


Fig. 6: XYZ image



Fig. 7: XYZ edge detected image



Fig. 8: YCbCr image

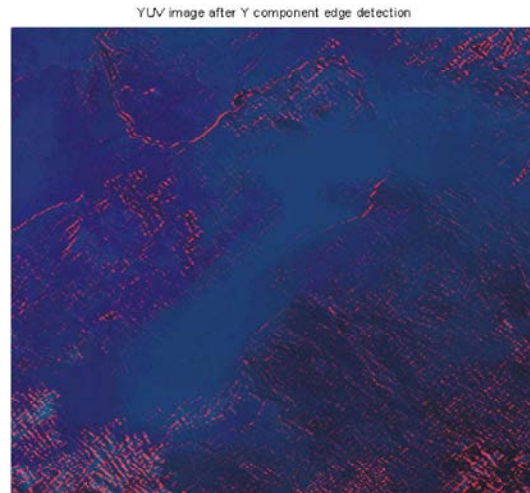


Fig. 11: YUV edge detected image



Fig. 9: YCbCr edge detected image

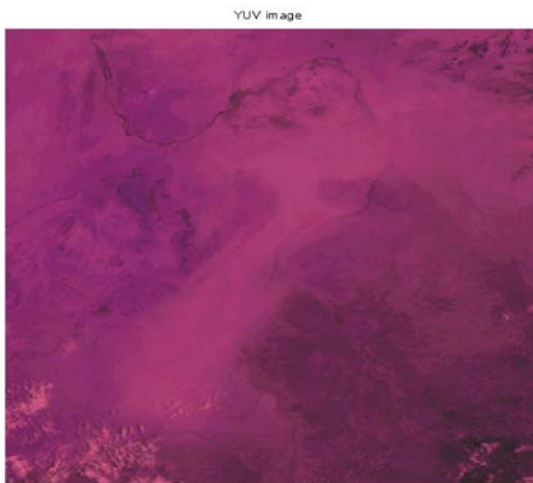


Fig. 10: YUV image

For RGB color model, The SSIM value range is around 0.62 and VIF value range is around 0.49. For XYZ color model, The SSIM value range is around 0.65 and VIF value range is around 0.55. For YcbCr color model, The SSIM value range is around 0.59 and VIF value range is around 0.54. For YUV color model, The SSIM value range is around 0.42 and VIF value range is around 0.62. From the dataset, XYZ model shows better quality of edge detection than the other color models. The original and edge detected RGB, YCbCr, YUV and XYZ images are shown below.

CONCLUSION

The proposed algorithm has a variety of applications especially in satellite images. Sobel operator and Laplacian operators are used to detect edges on different application specific satellite, biomedical and general color images. Also by changing RGB image to XYZ and YUV color space we ensure a better quality of satellite image with minimal data loss. Satellite images are considered as the key technique in remote sensing to investigate the land, ocean, cryosphere and atmosphere [13]. It also provides valuable information for finding area covered by cyclones or storms, clouds, vegetation, etc. Thereby improving the quality of satellite image opens new gates to the development of remote sensing applications. Therefore the concept of conversion of image from one color space to another extends hope to new horizons. The algorithm was developed based on RGB color space and the significant features extracted by converting it into YUV, YCbCr and XYZ models. Among these XYZ model shows better quality of edge detection.

REFERENCES

1. Gonzalez, R.C. and E. Woods, 2003. "Digital Image Processing" (Second Edition). New York: Prentice Hall, pp: 300-450.
2. Koschan, A., 1995. "A comparative study on color edge detection," in Proceedings of the 2nd Asian Conference on Computer Vision ACCV'95, pp: 574-578, Singapore.
3. Evans, A.N. and X.U. Liu, 2006. "A morphological gradient approach to color edge detection," IEEE Transactions on Image Processing, 15(6): 1454-1463.
4. Fan, J., W. Geref, M. Hacid, *et al.*, 2001. "An improved automatic isotropic color edge detection technique", Pattern Recognition Letters, 22(3): 1419-1429.
5. Naik, S.K. and C.A. Murthy, 2006. "Standardization of edge magnitude in color images", IEEE Transactions on Image Processing, 15(9): 2588 -2595.
6. Novak, C.L. and S.A. Shafer, 1987. "Color edge detection", Proc of DARPA Image Understanding Workshop, pp: 35-37.
7. Image Color Conversion, http://software.intel.com/sites/products/documentation/hpc/ipp/ippi/ippi_ch6/ch6_Intro.html.
8. Jeffrey C. Pommerville, 2010. "Alcama's Fundamentals of Microbiology", Jones & Bartlett Publishers.
9. Jill A. Engel-Cox, Christopher H. Holloman, Basil W. Coutant and Raymond M. Hoff, 2004. "Qualitative and quantitative evaluation of MODIS satellite sensor data for regional and urban scale air quality", Elsevier Journal of Atmospheric Environment, 38: 2004.
10. Sheikh, H.R., A.C. Bovik and L. Cormack, 2005. "Noreference quality assessment using natural scene statistics: JPEG2000", IEEE Transactions on Image Processing, 14(11): 1918-1927.
11. Qian, S. and G. Chen, 2010. "Four reduced-reference metrics for measuring hyper spectral images after spatial resolution enhancement" In: W. Wagner and B. Székely, (eds.): ISPRS TC VII Symposium – 100 Years ISPRS, Vienna, Austria, July 5-7, 2010, IAPRS, Vol. XXXVIII, Part 7A.
12. Sheikh, H.R. and A.C. Bovik, 2006. "Image information and visual quality", IEEE Transactions on Image Processing, 15(2): 430-444.
13. Image courtesy: Jeff Schmaltz, "LANCE/EOSDIS MODIS Rapid Response Team", NASA GSFC.